Facile layer-by-layer fabrication of semiconductor microdisk laser particles

Cite as: APL Photon. 8, 021301 (2023); doi: 10.1063/5.0130792
Submitted: 14 October 2022 • Accepted: 12 January 2023 •
Published Online: 1 February 2023

Paul H. Dannenberg,[1,2,3] Andreas C. Liapis,[1,2] Nicola Martino,[1,2] Debarghya Sarkar,[1,2] Kwon-Hyeon Kim,[1,2] and Seok-Hyun Yun[1,2,3,a)]

AFFILIATIONS

[1] Wellman Center for Photomedicine, Massachusetts General Hospital, Boston, Massachusetts 02114, USA
[2] Harvard Medical School, Boston, Massachusetts 02115, USA
[3] Harvard-MIT Health Sciences and Technology, Massachusetts Institute of Technology, Cambridge, Massachusetts 02139, USA

[a)] **Author to whom correspondence should be addressed:** syun@hms.harvard.edu

ABSTRACT

Semiconductor-based laser particles (LPs) with an exceptionally narrowband spectral emission have been used in biological systems for cell tagging purposes. The fabrication of these LPs typically requires highly specialized lithography and etching equipment and is typically done in a cleanroom environment, hindering the broad adoption of this exciting new technology. Here, using only easily accessible laboratory equipment, we demonstrate a simple layer-by-layer fabrication strategy that overcomes this obstacle. We start from an indium phosphide substrate with multiple epitaxial indium gallium arsenide phosphide layers that are sequentially processed to yield LPs of various compositions and spectral properties. The LPs isolated from each layer are characterized, exhibiting excellent optical properties with a lasing emission full width at half maximum as narrow as <0.3 nm and typical thresholds of ~6 pJ upon excitation using a 3 ns pulse duration 1064 nm pump laser. The high quality of these particles renders them suitable for large-scale biological experiments, including those requiring spectral multiplexing.

INTRODUCTION

Recently, the development of laser particles (LPs) has opened new avenues toward the study of biological systems. These particles are dispersible in aqueous solution, with micron-scale dimensions, and exhibit stable, sub-nanometer spectral linewidth emission.[1,2] These properties have enabled LPs to be used in cell tracking applications in tumor models,[3,4] cell sorting,[5] and intracellular cardiac sensing.[6] III–V semiconductor materials are well suited for microdisk LPs as their large refractive index, high quantum efficiency,[7] and high optical gain coefficients enable the creation of particles with dimensions on the order of 0.7 to 2 μm. Furthermore, by engineering the bandgap of the semiconductor materials, their emission can be tuned over a broad wavelength range, thus generating particles of many different colors.

The typical fabrication of microdisk LPs involves standard semiconductor fabrication steps: photolithography to create disk patterns on the wafer surface, plasma (dry) etching to transfer the patterns to the semiconductor, solution (wet) etching to remove disks from the wafer, and collection of the microdisk particles.[3] The lithography and dry etching are typically performed using specialized equipment available within a clean room in a semiconductor fabrication facility. Gaining access to these facilities is frequently challenging due to travel, training, and other logistic requirements. Therefore, we built a simple home-built setup within our lab using low-cost, minimally required tools to perform photolithography and wet etching. Controlled wet etching can create the disk patterns and release microdisks.[4] Using this setup, we were able to process InGaAsP/InP wafers and produce near-infrared (NIR) emitting LPs with comparable optical qualities to those made in our previous work at a centralized nanofabrication facility.[3]

For biological experiments, in which hundreds of thousands or even millions of cells must be tagged with multiple LPs, it is preferable to generate larger quantities of LPs. We have previously introduced a single multilayer wafer comprising multiple active layers of a gain material.[8] Conventionally, these layers are simultaneously patterned and etched using reactive ion etching (RIE) into columns consisting of stacks of microdisks. These stacks are broken

apart and released into an aqueous solution. This approach produces higher quantities of LPs (by multiple times) than a single-layer wafer. This batch processing, however, makes it difficult to isolate LPs arising from individual layers.

The wet-etching setup demonstrated in this paper, in addition to its logistical advantages, offers a convenient way to process multilayer wafers in a layer-by-layer manner so that LPs from each individual layer are patterned and released separately. The layer-by-layer fabrication strategy is similar to transfer printing, in which surface-patterned devices are transported to an alternative medium.[9] This technique has so far been used to incorporate III–V devices onto silicon or flexible substrates.[9–11] In some of these cases, the III–V semiconductor device is transferred to an alternative environment and the original wafer can be used to generate further devices. This multilayer technique is of great commercial importance since it enables substrate reuse of expensive III–V materials and does not require multiple epitaxial growth cycles interspersed with other wafer processing steps.[11] However, unlike previous work using transfer printing onto a solid substrate, the resultant environment in which the LPs are deposited is an aqueous one, enabling a simplified epitaxial transfer process free of an elastomeric stamp.

Here, we describe our novel layer-by-layer process to produce an aqueous dispersion of particles using a cyclical multilayer fabrication strategy. By starting from a three-layer parent wafer comprised of multiple active regions, we fabricate large quantities of microdisk LPs (>20 × 10^6 per sq cm) with excellent optical properties using easily accessible lab equipment.

RESULTS

Figure 1(a) shows photos of the home-built photolithography setup on a table and a wet-etching tube holder placed inside a chemical fume hood. The photolithography setup consists of a mask, a home-made 3D printed pressing jig (see the supplementary material, Note 2), and a UV lamp. After patterning, wet etching is performed in standard 5 to 15 ml beakers or tubes. Figure 1(b) illustrates the steps of the layer-by-layer fabrication strategy. The starting material consists of multiple epitaxial layers grown on an InP substrate (Xiamen Powerway Advanced Material Co., Ltd.). The active layers consist of $In_{1-x}Ga_xAs_yP_{1-y}$ and are separated by InP sacrificial layers. When growing monocrystalline layers spanning a total thickness several hundred nanometers, it is desirable to ensure that the grown layers are lattice matched to the indium phosphide substrate (lattice constant 5.87 Å). This occurs along a curve defined by x = y/(2.2–0.66 y).[12] Any of these combinations of x and y are permissible and enable the bandgap of each $In_{1-x}Ga_xAs_yP_{1-y}$ layer to be independently tuned anywhere across the 923–1666 nm range from InP (x = 0, y = 0) to $In_{0.53}Ga_{0.47}As$ (x = 0.47, y = 1). The starting material illustrated in Fig. 1(b) and used in our experiment has three active layers with different material compositions: $In_{0.75}Ga_{0.25}As_{0.54}P_{0.46}$ of thickness 200 nm (blue), $In_{0.65}Ga_{0.35}As_{0.74}P_{0.26}$ of thickness 220 nm (green), and $In_{0.60}Ga_{0.40}As_{0.90}P_{0.10}$ (pink) of thickness 240 nm, from top to bottom. The different thicknesses are chosen (see the supplementary material, Note 1) to ensure that the mode's effective refractive index scales appropriately with the specific alloy's emission wavelength. Interspersed between each active layer is 400 nm thickness of InP, which allows us to separate and thus isolate microdisk LPs produced from each active material. In practice, multilayered epitaxial growth of these materials is scalable with thicknesses of up to several hundred microns as previously demonstrated.[13]

To cyclically process each active material, a 1 μm coating of NR7-1000 negative tone photoresist was spun onto a chip roughly 1 × 1 cm^2 in size and baked on a hotplate at 150 °C for 1 min. A 4 × 4 $in.^2$ chrome mask was then placed on top of the chip [Fig. 1(a)]. The mask comprised of 2.5 μm circles in a hexagonal array with a center-to-center separation of 4 μm, resulting in a density of ~7 × 10^6 circles per sq cm. To ensure that the mask was placed in firm contact with the chip's surface, a 3D printed holder was used. By tightening the three wing nuts on the holder, the pressure between the mask and the chip could be increased as desired. We found that achieving a high degree of uniformity for such small features required careful positioning of the mask to ensure a flat surface across the chip. This was achieved by observing the shape of the Newton rings that formed at the mask/air/photoresist interface. The wing nuts were sequentially tightened or loosened until the rings became concentric with the chip's center, signifying that a flat interface between the mask and photoresist had been achieved. To expose the resist, a miniature i-line UV lamp was suspended ~4 in.

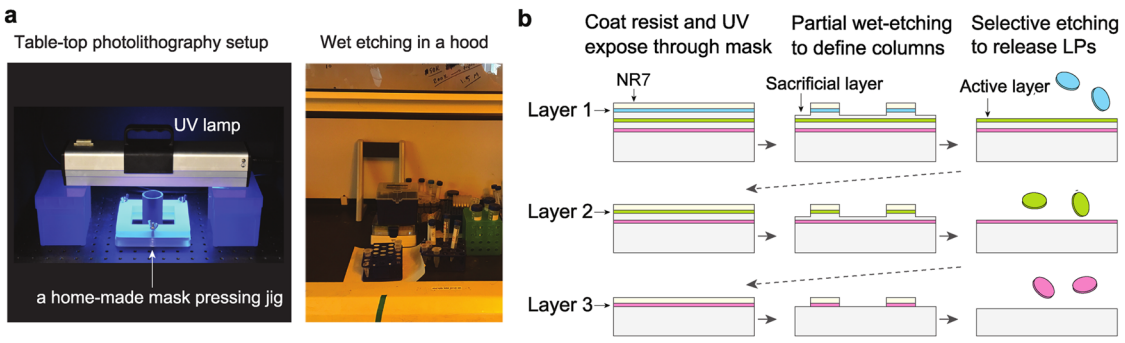

FIG. 1. Cyclical layer-by-layer fabrication of microdisk LPs from multilayer epitaxial assembly. (a) Photographs of the home-built UV photolithography setup (left) and wet etching tools (right). (b) Schematic of layer-by-layer fabrication producing batches of microdisk LPs from different active layers, 1 to 3, made of $In_{1-x}Ga_xAs_yP_{1-y}$.

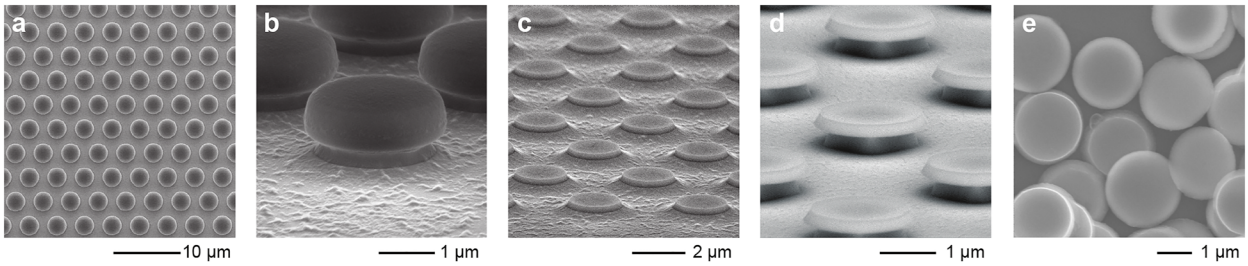

FIG. 2. Micrographs showing LPs at different points throughout the fabrication process. (a) 2.5 μm diameter circles of photoresist. (b) Wafer surface following wet etching in Br_2:HBr:H_2O. (c) Wafer surface following photoresist removal in acetone. (d) Microdisks still attached to the substrate after partial undercut in HCl. (e) Fully detached microdisks from the substrate.

from the mask surface (see the supplementary material, Note 2, for further details). We initially found that the formation of the photoresist features with a high degree of circularity was challenging due to spatial non-uniformities in the lamp's emission as well as the lack of a collimator. This arose due to the shape of the lamp, which was long and narrow (~30 × 8 cm^2), leading to the formation of ellipses instead of circles (Fig. S2). This problem was overcome using two solutions. First, a 1.25 × 2.3 $in.^2$ (diameter × height) tube was printed that acted as an iris, preventing oblique light rays from striking the sample. Second, the sample was rotated by 45° every 135 s during the total 18 min exposure. Following this, a 100 °C post-exposure bake for 1 min was performed followed by development in ~2.5% tetramethylammonium hydroxide (MF-319).

This resulted in circular photoresist features of ~2.5 μm in diameter [Fig. 2(a)]. The diameter could be well controlled by varying the exposure time. Next, the sample was briefly dipped in a 2:5:100 Br_2:HBr:H_2O solution for 5 s, which resulted in etching of the unmasked area of the topmost active layer. This wet chemical etching produces smaller InGaAsP microdisks of about 2 μm in diameter [Figs. 2(b)–2(d)]. The photoresist was then removed by a 3 min ultrasonication in acetone. A clear interface could be observed between the InP interlayer and InGaAsP. Microdisks were removed by submerging the chip upside down in 3:1 HCl:H_2O for 1 min under ultrasonication, which selectively targeted the InP while leaving the InGaAsP unaffected. Figure 2(d) shows the microdisks part of the way through this process before the LPs have been fully removed. This step uncovers the next active layer, while the LPs will detach into a liquid suspension after the InP has been fully undercut. The HCl liquid containing LPs was then diluted with ethanol, and the LPs were washed by three rounds of centrifugation, aspiration, and replacement with ethanol or deionized water. Following this, LPs can be transferred to an alternative substrate for characterization [Fig. 2(e)] or introduced into biological systems, or simply stored for later use in a 4 °C refrigerator in ethanol. Typically, the liquid handling process steps result in a yield of ~70% of the LPs that were originally patterned. This procedure was then repeated on the resultant parent wafer, which consisted of one fewer active layer material. This process allowed LPs comprised of different materials to be separately stored following each layer-by-layer round of processing.

After patterning and detaching LPs from each of the three InGaAsP active layers, we verified the success of our layer-by-layer transfer strategy by measuring the photoluminescence (PL) emission from the microdisks. The detached LPs from each active layer were transferred into separate glass-bottomed wells, before being fixed in position by a gel matrix (Corning Matrigel) of approximate refractive index 1.33. To measure their PL emission, a continuous wave 1064 nm laser beam focused to a spot size of ~2 μm diameter was swept across the sample and spectra measured at each 1.2 × 1.2 μm^2 pixel. A different characteristic PL spectrum was associated with particles found in each of the three wells, peaking at 1275, 1425, and 1575 nm, respectively [Fig. 3(a)]. An associated spectral image was constructed by assigning the wavelength of the spectral peaks to individual pixels when the peak height surpassed a threshold value. These images are shown in Fig. 3(b), with the threshold set to 80 counts. Each microdisk is represented by a cluster of pixels color

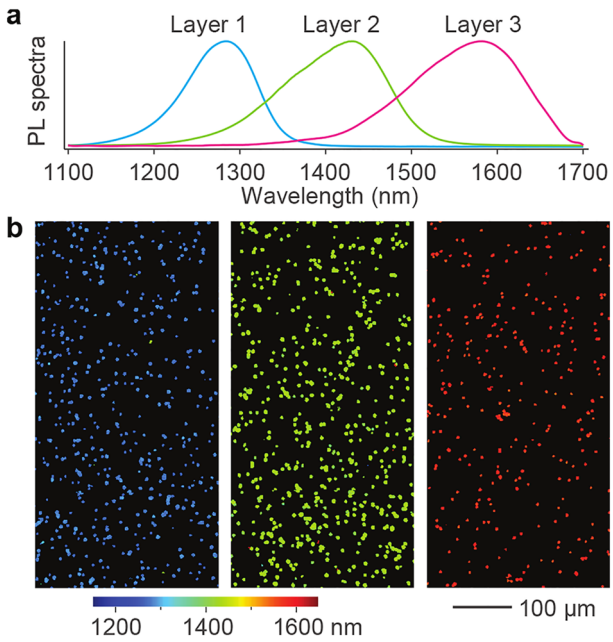

FIG. 3. Fluorescence properties of LPs obtained from the cyclical layer-by-layer processing. (a) Sample fluorescence spectra of a disk from the top InGaAsP layer, middle layer, and bottom layer from left to right. (b) Spatial maps showing the wavelength of the peak fluorescence emission from LPs in the glass-bottomed wells.

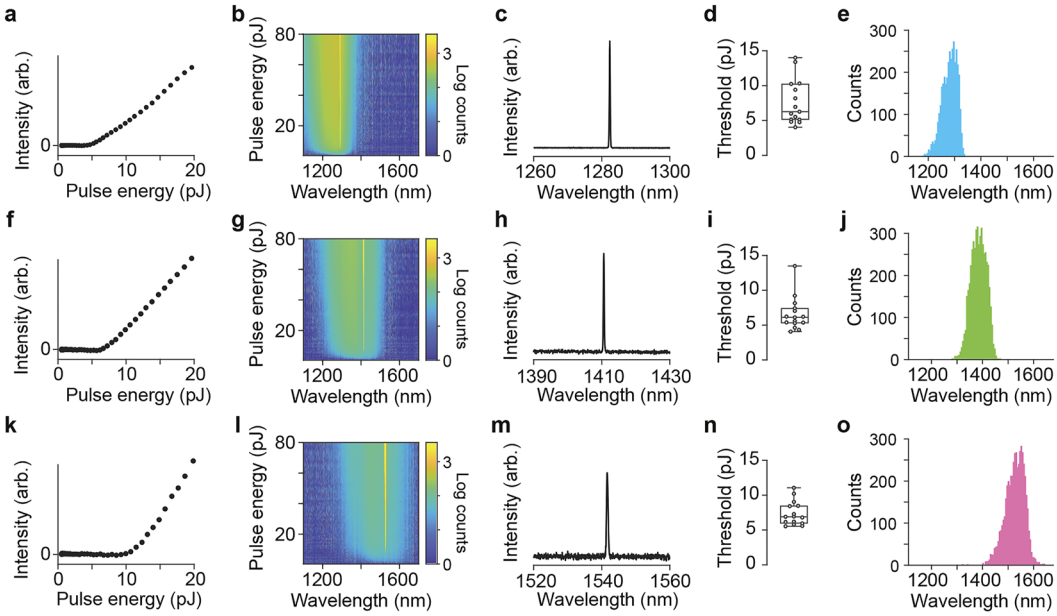

FIG. 4. Lasing properties of LPs obtained from the cyclical layer-by-layer processing from Layer 1 ($In_{0.74}Ga_{0.26}As_{0.56}P_{0.44}$) (a)–(e), Layer 2 ($In_{0.65}Ga_{0.35}As_{0.74}P_{0.26}$) (f)–(j), and Layer 3 ($In_{0.60}Ga_{0.40}As_{0.90}P_{0.10}$) (k)–(o). (a), (f), and (k) Energy in vs out curves of typical LPs obtained from each InGaAsP layer. (b), (g), and (l) Spectral irradiance at different pump pulse energies of typical LPs obtained from each InGaAsP layer. (c), (h), and (m) Sample high resolution spectra upon pumping each LP above threshold. (d), (i), and (n) Lasing thresholds of 15 LPs obtained from each layer. (e), (j), and (o) Histograms showing the distribution of lasing emission peaks from each layer.

coded by the wavelength of the peak PL emission at that location. The difference in wavelength found in each of the three wells shows that LPs were successfully obtained and isolated from each layer.

Next, we measured the lasing emission properties from LPs in each of the wells using a 1064 nm pulsed laser set to a 2 MHz repetition rate with 3 ns duration pulses. The pump laser was focused on individual microdisks, and the pulse energy steadily increased via the use of an acousto-optic modulator. The output intensity was measured by summing the counts across a spectral window gathered by a linescan camera attached to a spectrometer. For the well containing LPs comprised of $In_{0.74}Ga_{0.26}As_{0.56}P_{0.44}$, a distinct narrow linewidth peak as narrow as <0.3 nm typically appeared once the pulse energy exceeded the lasing threshold of each particle, which was found to be 5–15 pJ [Figs. 4(a)–4(d)]. These thresholds are comparable to those generated using a conventional fabrication strategy.[3] Measurements of the lasing distribution of 2000 disks were performed by rapidly scanning the pump laser across each sample using a pump pulse energy of 115 pJ and a camera pixel dwell time of 20 μs. Histograms showing the wavelength distributions of the LPs arising from $In_{0.74}Ga_{0.26}As_{0.56}P_{0.44}$ were then obtained [Fig. 4(e)], showing a distribution of lasing peaks between roughly 1200 and 1330 nm since the pulse energy exceeded threshold. LPs arising from the other InGaAsP compositions showed similar thresholds (6.6 pJ for $In_{0.65}Ga_{0.35}As_{0.74}P_{0.26}$ and 7.4 pJ for $In_{0.60}Ga_{0.40}As_{0.90}P_{0.10}$) but with different lasing emission wavelengths [Figs. 4(f)–4(o)]. For a given material, the wavelength range over which lasing occurs is determined by the gain bandwidth of the specific semiconductor material.

The LPs obtained separately from individual layers were coated with silica to enhance the stability of their optical properties[3] and introduced to HeLa cells in culture. After overnight incubation, LPs were fully internalized by the cells (Fig. 5) and could be distinguished by the lasing wavelength. This type of particle tagging can be used to simultaneously track tens of thousands of cells.[3]

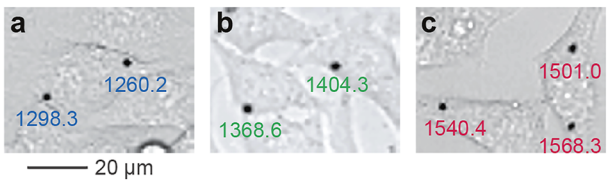

FIG. 5. Cell tagging with laser particles produced from different semiconductor layers [top layer to bottom layer (a) to (c)].

DISCUSSION

The layer-by-layer processing offers flexibility stemming from its ability to produce batches of LPs with separate gain materials all from a single growth run on a single parent wafer. First, the ability to separate LPs that exhibit different emission properties enables different LP types to be introduced to different cell populations. This may enhance future experiments by enabling increased assay flexibility. Second, this technique could be useful during the optimization of the LP materials, since several different designs and compositions can be tested on a single wafer substrate. For example, we have demonstrated the fabrication of microdisks of both different

thicknesses and different material compositions. More complex designs involving a cladded structure or quantum wells may be produced and then evaluated all from the same parent wafer.[14,15] Importantly, each different type of LP can be isolated and tested individually. This approach could prove particularly useful in evaluating the effects of different LP alloys and microdisk sizes on biological systems.

Another advantage of the layer-by-layer fabrication is the additional degree of freedom it affords in altering the size of LPs for a given multilayer wafer. By varying the exposure duration while processing each active layer, the diameters of the resultant LPs can be independently altered within each layer. When a single, deep plasma etching step was used, we were unable to independently vary the diameters of the LPs arising from each layer since the diameters of microdisks from all layers were determined by the photoresist mask diameter.[8] Alternatively, the layer-by-layer production could be used to alter the properties of each LP layer as it is produced. For example, nanoparticles have been added to the surface of microdisk LPs to enhance omnidirectional emission[16] and metallo-dielectric layers have been introduced to enhance mode confinement.[17] Such depositions are applied only to the wafer surface and so can only be adapted for use in situations in which each active material is exposed in a layer-by-layer fashion. For example, by adding nanoparticles to its surface, the directional nature of the LPs' emission, which is predominantly radial, can be rendered more isotropic, which has been shown to enhance the signal strength of LPs during cell tracking.[16]

Additionally, the layer-by-layer production can produce large numbers of LPs with relative ease and low financial cost. Indeed, the use of a multilayer parent wafer as opposed to multiple single layer wafers has previously been shown to be cost effective (see the supplementary material, Note 3).[11] The quantity of LPs that can be generated from each parent wafer scales with the number of layers. Here, we have demonstrated the production of ~7×10^6 LPs per layer per sq cm. The fabrication strategy entails only modest, widely available equipment requirements: a spin coater, chemical hood, hot plate, handheld UV lamp, and some 3D printed parts. Until now, a significant disadvantage of semiconductor LP technology is that it requires access to a nanofabrication facility. Indeed, past fabrication strategies have frequently relied on electron-beam lithography,[4,15] plasma etching technologies,[3,15] or other high-end equipment usually only found in shared, core facilities. Access to these facilities can often be logistically challenging and expensive and require lengthy training procedures to gain access to equipment shared between multiple users and research teams. The simple low-cost setup we have demonstrated could be useful for many labs with limited resources or access to high-end equipment, especially in early rapid design and prototyping stages.

Our layer-by-layer method demonstrated a high degree of uniformity, producing only a negligible fraction of non-lasing LPs. Notably, the technique can be used without access to a cleanroom. Indeed, all steps were performed in a standard lab fume hood except for the UV exposure, which took place outside the hood. While we did not encounter significant issues with contamination by dust due to the small size of our chips (1×1 cm^2), it is important to note that, if larger chips were to be used, a clean box might still be desirable. However, the layer-by-layer technique is resilient to contamination by small defects since etching under ultrasonication of the sacrificial layers, used to detach successive layers of LPs, also lifts off and removes small dust particles or LPs from a prior layer that have re-adhered (Fig. S3), preventing them from propagating defects to subsequent layers.

CONCLUSIONS

In conclusion, we have developed a convenient, flexible layer-by-layer nanofabrication method that we have used to produce single-mode microdisk LPs that can be freely dispersed in an aqueous suspension. Different epitaxial layers in the original wafer can correspond to different LP designs, which can be isolated and chosen for use in a particular experiment as desired. Therefore, such a technique enables a high degree of flexibility: LPs originating from specific layers can be selectively introduced into alternative inorganic or biological systems. Our measurements reveal average lasing thresholds below 10 pJ, suggesting a high degree of circularity and low surface roughness. This low threshold renders the particles well suited to imaging applications. Importantly, our nanofabrication strategy avoids the use of much sophisticated equipment, and we expect that it will broaden the study of epitaxially grown semiconductor lasers as liquid-dispersible particles.

SUPPLEMENTARY MATERIAL

More details of the effective mode refractive index, the lithography setup, wafer cost analysis, and further fabrication details can be found in the accompanying supplementary material.

ACKNOWLEDGMENTS

This study was supported by the US National Institutes of Health (Grant Nos. DP1-OD022296 and R01-EB033155). P.H.D. also acknowledges the funding from the Harvard University Presidential Scholars Fund.

AUTHOR DECLARATIONS

Conflict of Interest

P.H.D., N.M., and S.H.Y. hold patents on laser particle technologies. N.M., A.C.L., and S.H.Y. have financial interest in LASE Innovation Inc., a company focused on commercializing technologies based on laser particles. The financial interest of N.M. and S.H.Y. was reviewed and are managed by Mass General Brigham in accordance with their conflict-of-interest policies.

Author Contributions

Paul H. Dannenberg: Conceptualization (lead); Data curation (lead); Formal analysis (lead); Investigation (lead); Methodology (lead); Project administration (equal); Software (supporting); Validation (lead); Visualization (equal); Writing – original draft (lead); Writing – review & editing (equal); **Andreas C. Liapis**: Data curation (supporting); Methodology (supporting); Software (equal); Writing – review & editing (equal). **Nicola Martino**: Data curation (supporting); Software (equal); Writing – review & editing (supporting). **Debarghya Sarkar**: Data curation (supporting); Investigation (supporting); Methodology (supporting); Writing – review

& editing (supporting). **Kwon-Hyeon Kim**: Data curation (supporting); Investigation (supporting). **Seok-Hyun Yun**: Data curation (equal); Funding acquisition (lead); Project administration (equal); Resources (lead); Supervision (lead); Writing – original draft (supporting); Writing – review & editing (equal).

DATA AVAILABILITY

The data that support the findings of this study are available from the corresponding author upon reasonable request.

REFERENCES

[1]M. Humar and S. H. Yun, Nat. Photonics **9**, 572 (2015).
[2]M. Schubert, A. Steude, P. Liehm, N. M. Kronenberg, M. Karl, E. C. Campbell, S. J. Powis, and M. C. Gather, Nano Lett. **15**, 5647 (2015).
[3]N. Martino, S. J. J. Kwok, A. C. Liapis, S. Forward, H. Jang, H.-M. Kim, S. J. Wu, J. Wu, P. H. Dannenberg, S.-J. Jang, Y.-H. Lee, and S.-H. Yun, Nat. Photonics **13**, 720 (2019).
[4]A. H. Fikouras, M. Schubert, M. Karl, J. D. Kumar, S. J. Powis, A. Di Falco, and M. C. Gather, Nat. Commun. **9**, 4817 (2018).
[5]P. H. Dannenberg, J. Kang, N. Martino, A. Kashiparekh, S. Forward, J. Wu, A. C. Liapis, J. Wang, and S.-H. Yun, Lab Chip **22**, 2343 (2022).
[6]M. Schubert, L. Woolfson, I. R. M. Barnard, A. M. Dorward, B. Casement, A. Morton, G. B. Robertson, P. L. Appleton, G. B. Miles, C. S. Tucker, S. J. Pitt, and M. C. Gather, Nat. Photonics **14**, 452 (2020).
[7]Y. Takanashi and Y. Horikoshi, Jpn. J. Appl. Phys. **20**, 1271 (1981).
[8]P. H. Dannenberg, A. C. Liapis, N. Martino, J. Kang, Y. Wu, A. Kashiparekh, and S.-H. Yun, ACS Photonics **8**, 1301 (2021).
[9]H. Yang, D. Zhao, S. Chuwongin, J.-H. Seo, W. Yang, Y. Shuai, J. Berggren, M. Hammar, Z. Ma, and W. Zhou, Nat. Photonics **6**, 615 (2012).
[10]J. Justice, C. Bower, M. Meitl, M. B. Mooney, M. A. Gubbins, and B. Corbett, Nat. Photonics **6**, 612 (2012).
[11]J. Yoon, S. Jo, I. S. Chun, I. Jung, H.-S. Kim, M. Meitl, E. Menard, X. Li, J. J. Coleman, U. Paik, and J. A. Rogers, Nature **465**, 329 (2010).
[12]S. Seifert and P. Runge, Optical Materials Express **6**(2), 629–639 (2016).
[13]M. G. Mauk, A. N. Tata, and J. A. Cox, J. Cryst. Growth **225**, 236 (2001).
[14]M. Athanasiou, R. M. Smith, J. Pugh, Y. Gong, M. J. Cryan, and T. Wang, Sci. Rep. **7**, 10086 (2017).
[15]Z. Zhang, L. Yang, V. Liu, T. Hong, K. Vahala, and A. Scherer, Appl. Phys. Lett. **90**, 111119 (2007).
[16]S.-J. Tang, P. H. Dannenberg, A. C. Liapis, N. Martino, Y. Zhuo, Y.-F. Xiao, and S.-H. Yun, Light Sci. Appl. **10**, 23 (2021).
[17]M. P. Nezhad, A. Simic, O. Bondarenko, B. Slutsky, A. Mizrahi, L. Feng, V. Lomakin, and Y. Fainman, Nat. Photonics **4**, 395 (2010).